AUDITOR – GA 687367

Advanced Multi-Constellation EGNSS Augmentation and Monitoring Network and its Application in Precision Agriculture

D5.2 Version 1.0

GNSS Network processing software implementation and test

Contractual Date of Delivery:	M16 (End Apr, 2017)
Actual Date of Delivery:	15th May, 2017
Editor:	UPC
Author(s):	Manuel Hernández-Pajares, Alberto García-Rigo, David Roma-Dollase, Haixia Lyu and Victoria Graffigna (UPC).
Work package:	*WP5 – Network software for GNSS*
Security:	**CO**
Nature:	**R**
Version:	1.0
Total number of pages:	38

Abstract:

This document is an evolution of the network part of D4.1 and D5.1, focusing on the new updates in the design of iBOGART network modules. It also covers aspects on the implementation for each of the modules as well as results on their verification/validation in emulated real time conditions.

Document Control

Version	Details of Change	Author	Approved	Date
0.1	Document Created	All	-	13/04/2017
0.2	First version distributed	AGR	-	14/04/2017
0.3-0.9	Internal iterations	MHP, AGR	-	26/04/2017
1.0	Consolidated version	MHP, AGR	MHP/AGR	15/05/2017

Executive Summary

This document addresses the updates in the implementation and testing of iBOGART network modules. It is important to remark that this document is an evolved version of section 2 in D4.1 Version 0.6 iBOGART design, implementation and validation and of the former deliverable D5.1. In this way, there are parts replicated from D5.1 that serve as background for the new work carried out on implementation for each of the modules as well as results on their verification/validation before integration.

The document is divided in several sections covering the above points on: (1) the iBOGART-net-MODEL real time data acquisition, (2) TOMION's SW pre-processing modules, (3) TOMION's SW prefit module, (4) TOMION's SW filter module and (5) Communication aspects between the Central Processing Facility (CPF) and the user GNSS receivers.

It shall be remarked that the integration of the different modules will be carried out within WP6 as well as the overall tests under actual real time conditions.

Authors

Partner	Name	e-mail
UPC	Manuel Hernández-Pajares	e-mail: manuel.hernandez@upc.edu
	Alberto García Rigo	e-mail: alberto.garcia.rigo@upc.edu
	David Roma Dollase	e-mail: droma@el.ub.edu
	Haixia Lyu	e-mail: haixia.lyu@upc.edu
	Victoria Graffigna	e-mail: victoria.graffigna@estudiant.upc.edu

Table of Contents

List of tables

List of Figures

List of Acronyms and Abbreviations

Term	Description
BNC	BKG Ntrip Client
BS	B-spline
CPF	Central Processing Facility
dSTEC	Differential STEC
GIM	Global Ionospheric Maps
GNSS	Global Navigation Satellite System
GUI	Graphical User Interface
KPI	Key Performance Indicator
MSTID	Medium Scale TID
NABS	Non-uniform Adaptive B-splines
NTRIP	Network Transport RTCM via Internet Protocol
PVT	Position-Velocity-Time
RMS	Root Mean Square

RT	Real Time
RTK	Real Time Kinematic
SH	Spherical Harmonic
SSR	RTCM's State Space Representation
STEC	Slant TEC
SW	Software
TEC	Total Electron Content
TID	Travelling Ionospheric Disturbance
TOMION	TOmographic Model of the IONosphere
UPC	Universitat Politècnica de Catalunya
VTEC	Vertical TEC
WARTK	Wide Area RTK
ZTD	Zenith Tropospheric Delays

1. Introduction

In order to enable AUDITOR users to have precise positioning at a low cost in the field of precise agriculture/farming, dedicated network and user algorithms are being implemented based on Wide Area Real Time Kinematic (WARTK) as well as on precise (near) real time determination of the ionospheric state by means of the RT version of the TOMION software [1]. In the overall architecture (see Figure 1.1), the network algorithms are being implemented as part of the IBOGART Cloud and the user algorithms have an impact on the Network Software within the Zynq board.
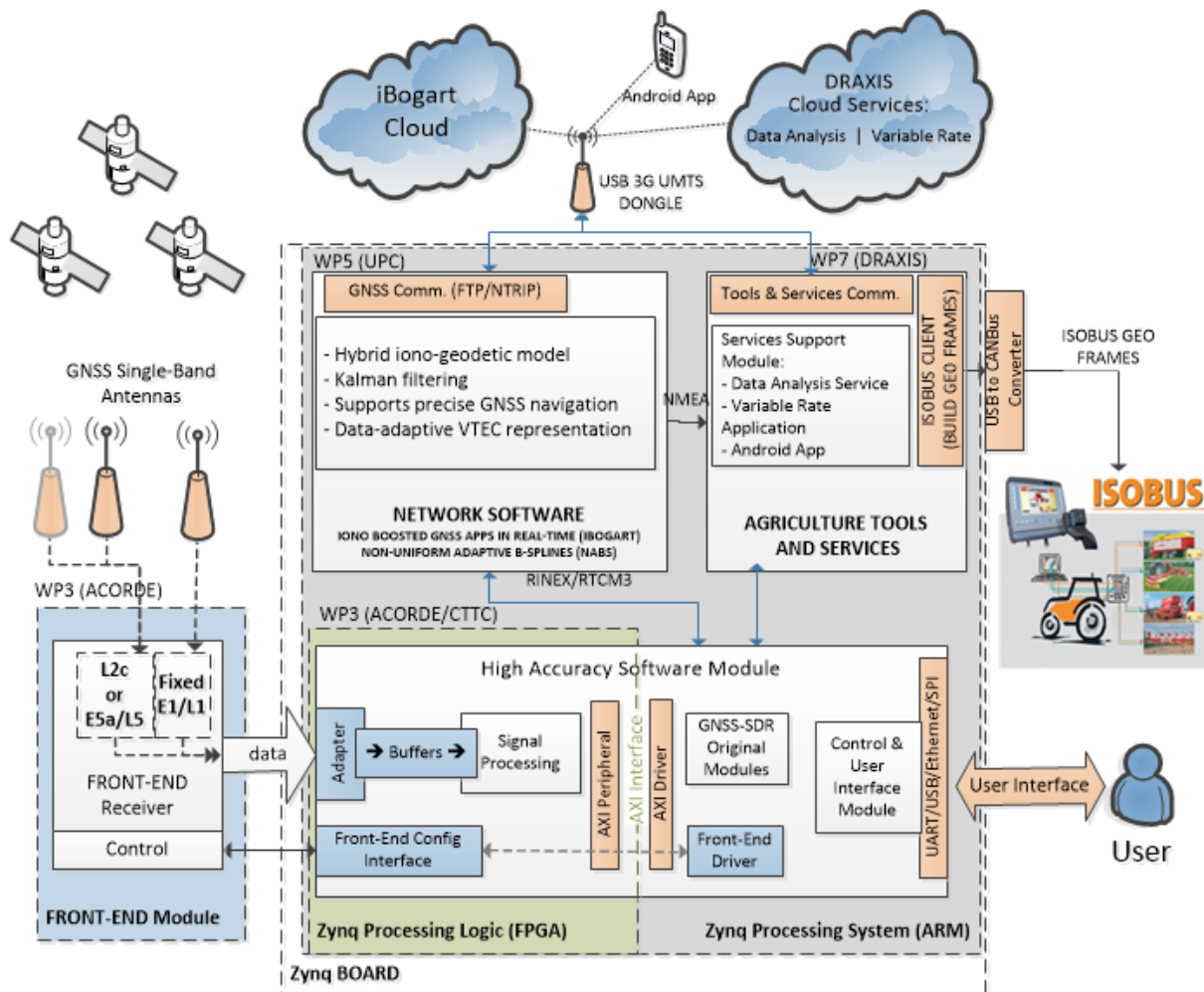
Figure 1.1: System Architecture (updated w.r.t. to D2.2)

In brief, a new server –chapman.upc.es- has been installed to address all real time processes within UPC-IonSAT, including AUDITOR Central Processing Facility (CPF). The iBOGART data acquisition algorithms based on BNC third-party open source Software have been renewed to support a higher number of datastreams being gathered simultaneously, to diminish the latencies for any AUDITOR potential user, as well as to implement more efficient recovery tools. In addition, the iBOGART-net-model has been installed in the new server and minor changes have been necessary to allow for TOMION SW continuous real-time execution (the ionospheric part). In addition, the geodetic part has been improved as well to be used in AUDITOR's operational scenario where tests shall be performed.

2. iBOGART-net-MODEL: adopted iBOGART-net architecture

2.1 CPF overall architecture

In brief, the Central Processing Facility is part of the so-called iBOGART Cloud, which has been implemented at UPC premises (see D2.1 Architecture Design). The CPF will offer a passive service, computing and distributing AUDITOR corrections through the Internet to any potential AUDITOR user (mainly targeting South-East Europe) and mainly based on GPS L1 and L2frequencies. For this purpose, a unidirectional link from the CPF is needed to distribute the corrections to any interested AUDITOR user.

The CPF is running in *chapman.upc.es* server, and all the different modules being updated (mainly the RT-GNSS data gathering, the preprocessing, the prefit and the filter modules) have been consolidated. The provision of corrections at AUDITOR region of interest is now feasible and about to be operational, after checking that the integration of the modules (to be done within WP6) is working as expected in actual real time conditions.

The overview of the main components of the CPF and AUDITOR dissemination can be visualized in Figure 2.1 and Figure 2.2.
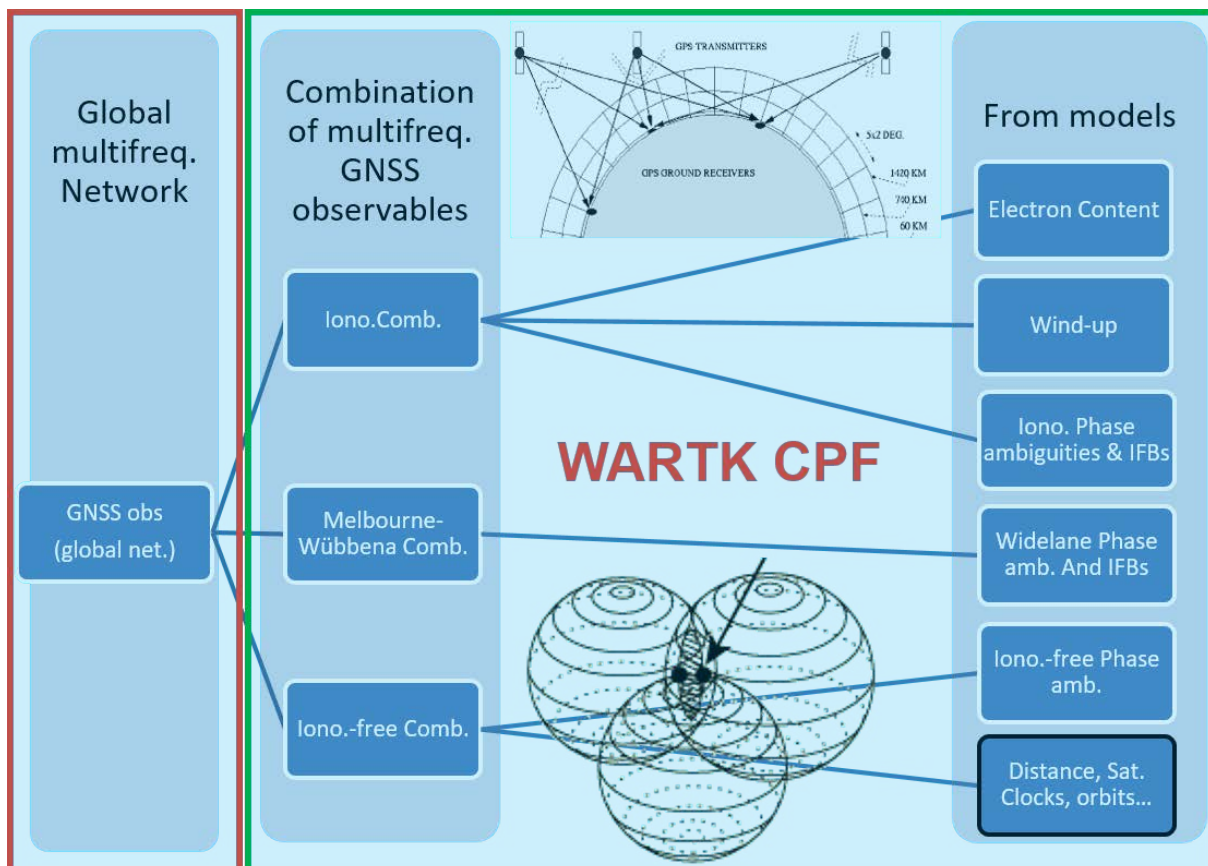
Figure 2.1: RT-GNSS data gathering module (marked in red) and the CPF core (in green), which implements the prefit and filter modules.
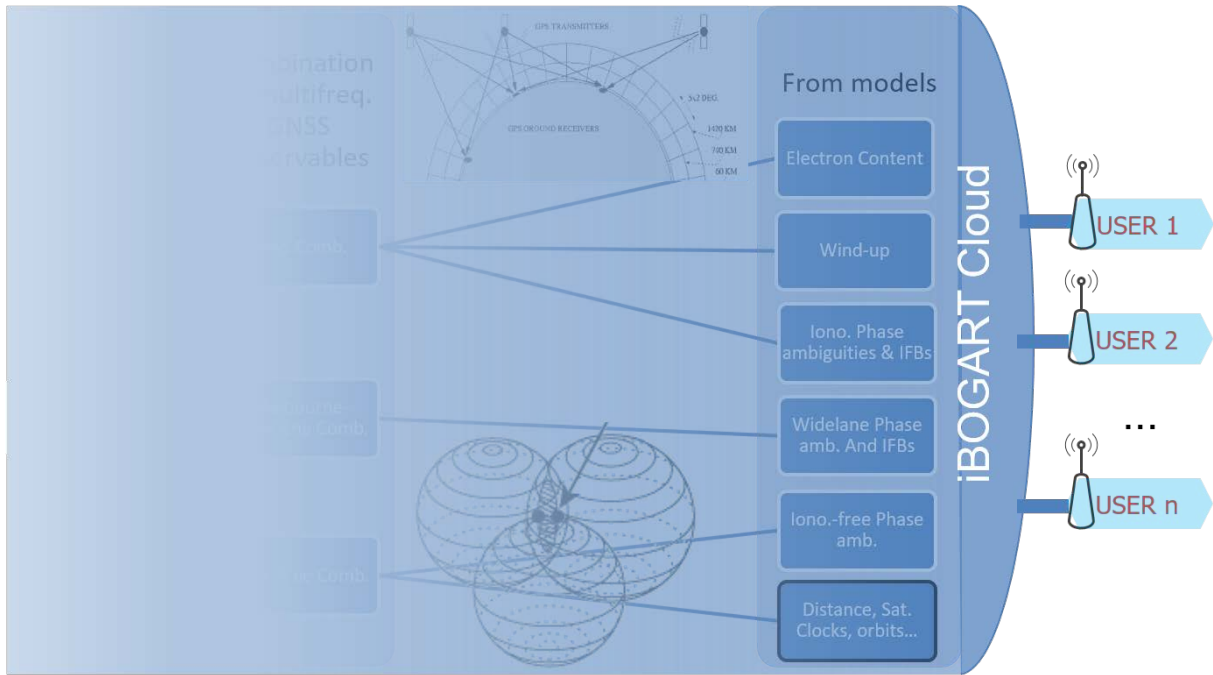
Figure 2.2: Dissemination of iBOGART corrections to AUDITOR users.

More in detail, the software modules of TOMION's SW running WARTK for AUDITOR, i.e. the so-called hybrid ionospheric-geodetic model, can be seen in Figure 2.3 (also, please refer to deliverable D2.2. Subsystem specification).
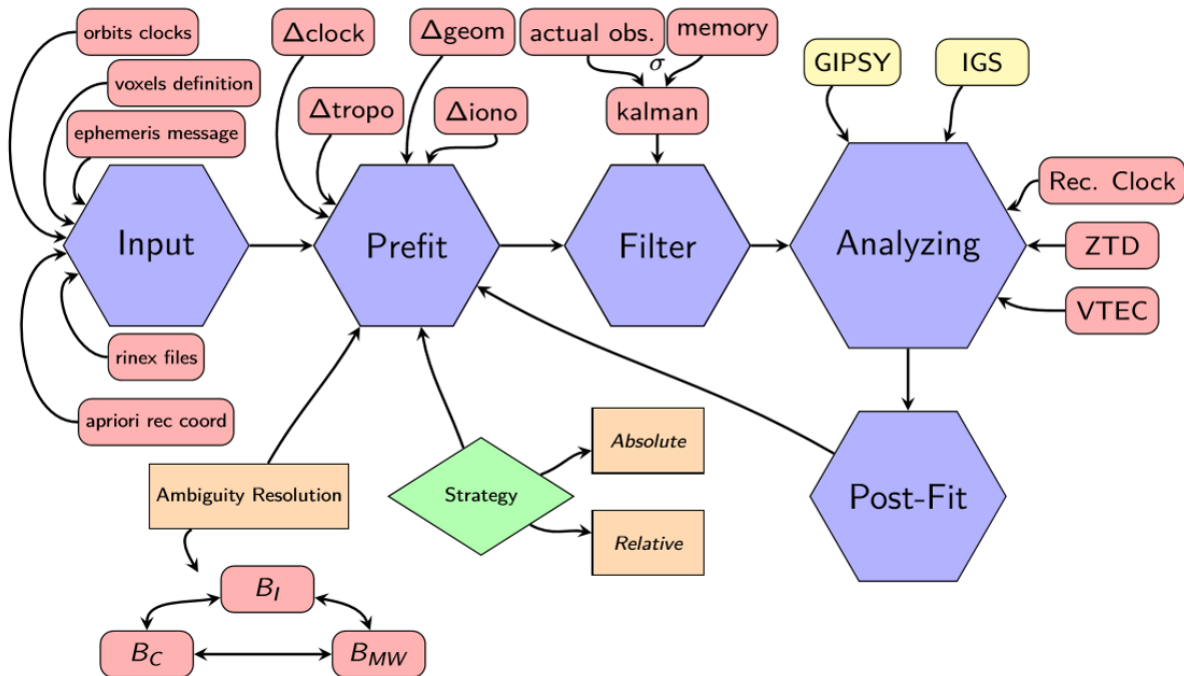
Figure 2.3: Hybrid ionospheric-geodetic approach components.

In brief, several updates have been performed on the following aspects:

- The Ocean Tidal Loading model and antenna phase centers.

- The tropospheric mapping function and a priori ZTD.

- A new ambiguity fixing scheme, with the actual removal of the corresponding carrier phase biases instead of constraining them.

- The relative processing has been improved:

    o By assuring the consistency of the internal satellite clock estimation at the CPF, mainly from the reference receiver measurements.

    o By removing out small outliers, which are identified in the post-fit residual signature (and in the ZTD estimation).

- Additional external references have been added, in particular by means of GIPSY/OASIS-II JPL software to assess ZTD in post-processing mode.

The following sections cover the real time acquisition SW (TOMION's input module) from the design and implementation point of view as well as from its performance evaluation (Section 2.2). In addition, Sections 2.4 and 2.5 (on prefit and filter modules, respectively) cover the above-mentioned updates, the implementation of TOMION's hybrid approach in the new dedicated server and associated evaluation tasks carried out. Finally, a section covers the discussion on format and dissemination of corrections to the users (Sections 2.9).

2.2 RT-GNSS data gathering module – consolidated design and implementation

2.2.1 Introduction

From the pre-AUDITOR data gathering module, a set of improvements have been carried out to go a step forward on stability and capacity to enable handling multiple datastreams in parallel. In particular, improvements such as: (1) a new bash script to start BNC, implementing an automatic restart mechanism in case being down, (2) a new script to pre-process BNC's observations in Python (3) the increase of the number of open datastreams (and public NTRIP broadcasters accessible at no cost by registration), (4) the update on datastreams' selection algorithm to be more flexible in the way to select streams (for instance, considering a minimum baseline between stations to be retrieved), (5) rebuild BNC's configuration file with the latest available data before its execution, (6) new mechanism to implement a waiting time threshold to minimize latency, (7) update of BNC software to the latest version, (8) lower memory allocation of the system when running, and (9) running two instances in parallel to cover both the global scale and AUDITOR test region at Greece and the surrounding area.

2.2.2 Design and implementation details

The real time acquisition software is based on the data provided by public casters distributing reference station data through NTRIP (Network Transport RTCM via Internet Protocol). The core element of this block is the BKG Ntrip Client (BNC; see Figure 2.3), version 2.12.3. BNC connects to a set of selected casters that distribute the observables of different stations. Then, this information is synchronized epoch by epoch from all stations and sent to a single file.

In the case of the global network of receivers, BNC is configured to output data with a sampling rate of 10 seconds with a latency of 10 seconds for synchronizing the input data of the casters. If any data is received afterwards, it is discarded.
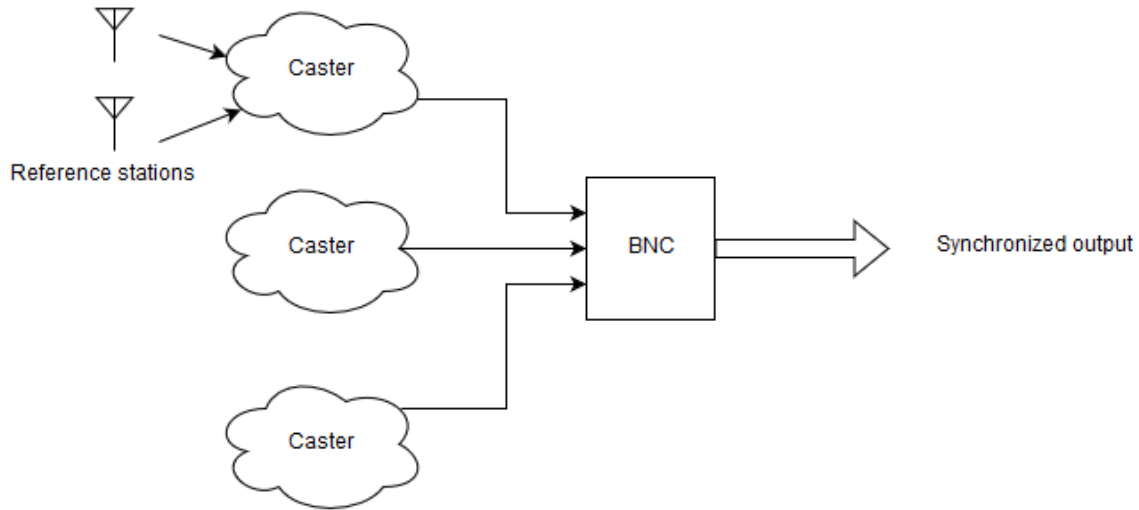
Figure 2.4: Real Time acquisition software block diagram

This updated software has been running since beginning of autumn 2016 without any relevant issues on the new dedicated server, chapman.upc.es, providing data up to 300 reference stations worldwide, including 48 permanent stations in Europe, useful for AUDITOR purposes (see Figure 2.2).
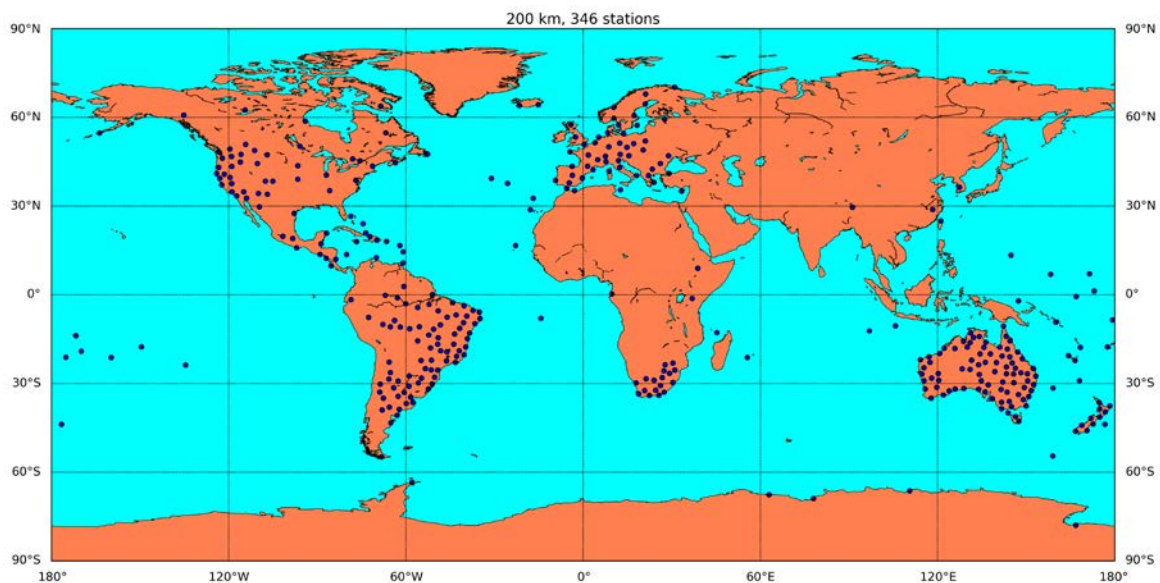
Figure 2.5: Considering a minimum distance of 200 km, a total of up to 346 NTRIP GNSS datastreams are selected for their acquisition.

In addition, a densified network within Greece and its surrounding area has been considered as well for testing purposes. In this case, the minimum allowed separation between selected reference GNSS stations has been set to zero and a total of 16 available datastreams have been selected from four different NTRIP casters (4 datastreams from euref-ip.asi.it, 7 from ntrip.pecny.cz, 4 from www.euref-ip.net and 1 from igs-ip.gmv.com). These can be seen in Figure 2.6 as well as Figure 2.9. An independent BNC instance has been running for this specific network from end of October, 2016. In this case, a

waiting time of 2 seconds and a sampling rate of 1 Hz have been considered. Note that these values can be modified if necessary at the CPF side. In case the wait time is diminished, the latency would decrease but it would imply losing the observations not fulfilling the required latency threshold.

Figure 2.6: Considering a minimum distance of zero kilometers, 16 NTRIP GNSS datastreams are selected in Greece and its surrounding area for their acquisition at 1 Hz.
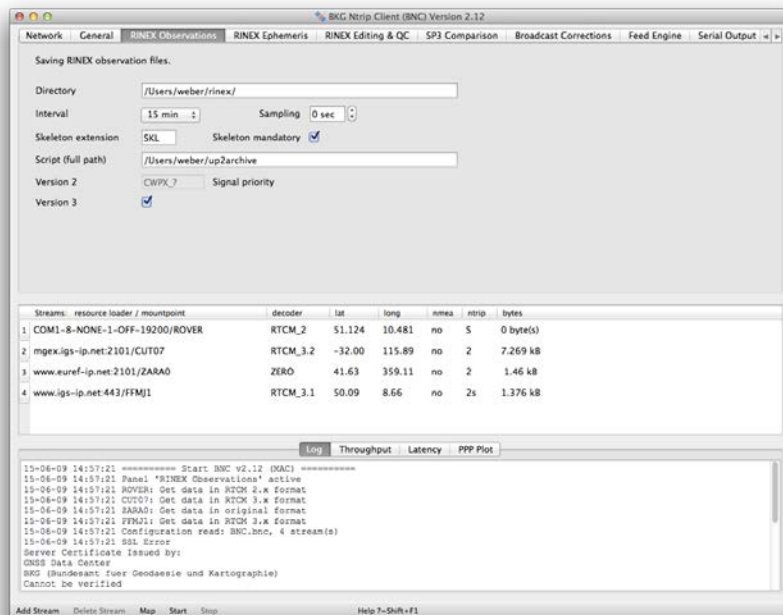
Figure 2.7: Example of BNC executed in a pop-up window. Nonetheless, in AUDITOR CPF, the adopted solution is based on command line tools.

2.3 RT-GNSS data gathering module – performance verification

2.3.1 Introduction

To ensure stability and reliability of this part, a set of scripts have been developed. These scripts continuously monitor the BNC process and if it is stopped for any reason, BNC is automatically restarted. This usually produces a maximum downtime of 30 seconds before full recovery after such rare event.

The output file is also continuously being monitored to validate the number of reference stations from which we receive data. In case the daily mean value goes below a defined threshold (currently set to 200 stations), a second script will be executed to reconnect a reasonable number of reference stations. This script will then connect to all the casters defined in an xml file and collect the set of available stations for each of them. Afterwards, BNC is executed for them in groups of 300 stations with the same timing configurations than above mentioned. Then, taking into account the output file generated and the information stored from previous runs of these scripts, they are classified in terms of availability and latency. Finally, a subset of the best casters/reference stations is selected taking into account a minimum distance between them (currently set to 300 km). The result of this script is a new BNC configuration file with a new set of reference stations with a minimum distance of 300 km and with the lowest latency and maximum availability. This new configuration file will be automatically reloaded by BNC at the beginning of the next day.

In the continuous testing performed so far, for estimating real-time Global Ionospheric Maps, the output latency of the acquisition has been verified showing that the outputs are always generated at the given latency (10 or 2 seconds).

Depending on network load, casters workload and other parameters that cannot be controlled, it is expected that the number of data streams will be lower since more of them will be discarded. In any case, BNC ensures that the latency of the accepted observations will never be higher than 10 seconds in the global case and 2 seconds in the AUDITOR test region.

The verification test has been performed in terms of the following Key Performance Indicators: Timeliness of the input data to the CPF iBOGART input module and Availability of datastreams. In this context, the following thresholds have been adopted to test the obtained KPIs:

Timeliness thresholds:

    critical threshold over 2 seconds (over 10 seconds in the global run)

    acceptance 2 seconds (10 seconds in the global run)

    over-performance 1 second (below 10 in the global run)

Availability thresholds:

> critical threshold 50%
>
> under-performance 75%
>
> acceptance 90%
>
> over-performance 99%

Note that the verification of correct data acquisition in terms of the number of available reference stations is also part of the validation of the tests: "iBOGART-net-MODEL: Post-processing" (see Table 6.49 in D1.3), "iBOGART-net-MODEL: Real-time" (see Table 6.50 in D1.3) and AUDITOR's Message generation and retrieval test (see Table 6.51 in D1.3). In this last case, the latency shall also be estimated as part of the calculation of the latency of the corrections.

2.3.2 Test carried out

The results for a more than three weeks' period have been analysed with actual real time conditions, for day of year 304 to 326, 2016. It is important to remark that this test has been conducted in actual real time conditions.

Regarding the evaluation of the Timeliness KPI, the module directly discards samples with latencies over two seconds as a measure to avoid further delays, which could imply providing corrections with an unacceptable delay to users. In this way, the imposed wait time of two seconds makes that all accepted observations are processed in two seconds without penalizing significantly the availability KPI (see below). In this way, the Timeliness of the accepted observations meets the acceptance threshold defined in previous subsection.

Regarding the evaluation of the Availability KPI in the period being analysed, note that the positive counting is determined only in case the observations are available and the above-mentioned timeliness threshold is fulfilled. More in detail, the availability considering all epochs for the test period is depicted in Figure 2.8, showing more clearly (due to the adopted point size) the epochs where there is a lack of data.
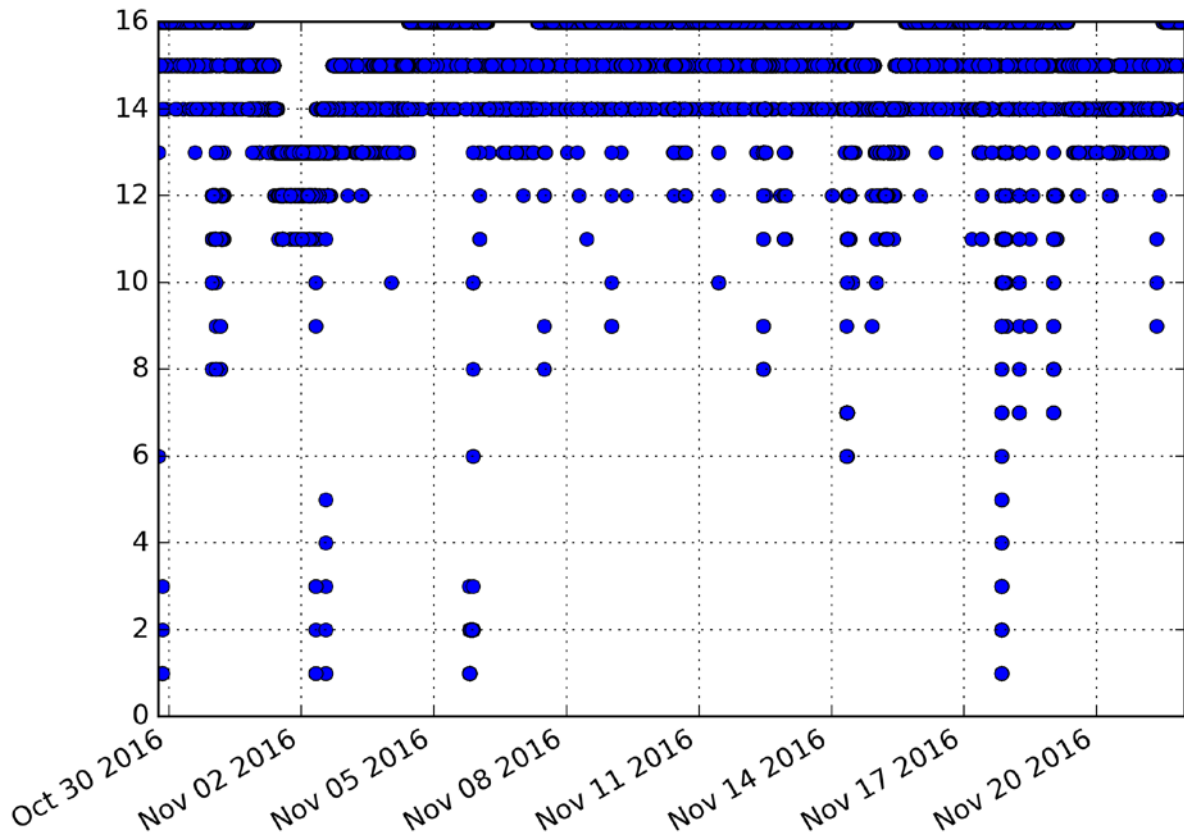
Figure 2.8: Availability test on the global GNSS RT acquisition for days 303 to 326.

In addition, Figure 2.9 shows the same availability test but distinguishing between the datastreams of each NTRIP broadcaster being considered for the AUDITOR network of RT-GNSS receivers in Greece

and   its   surrounding   area.
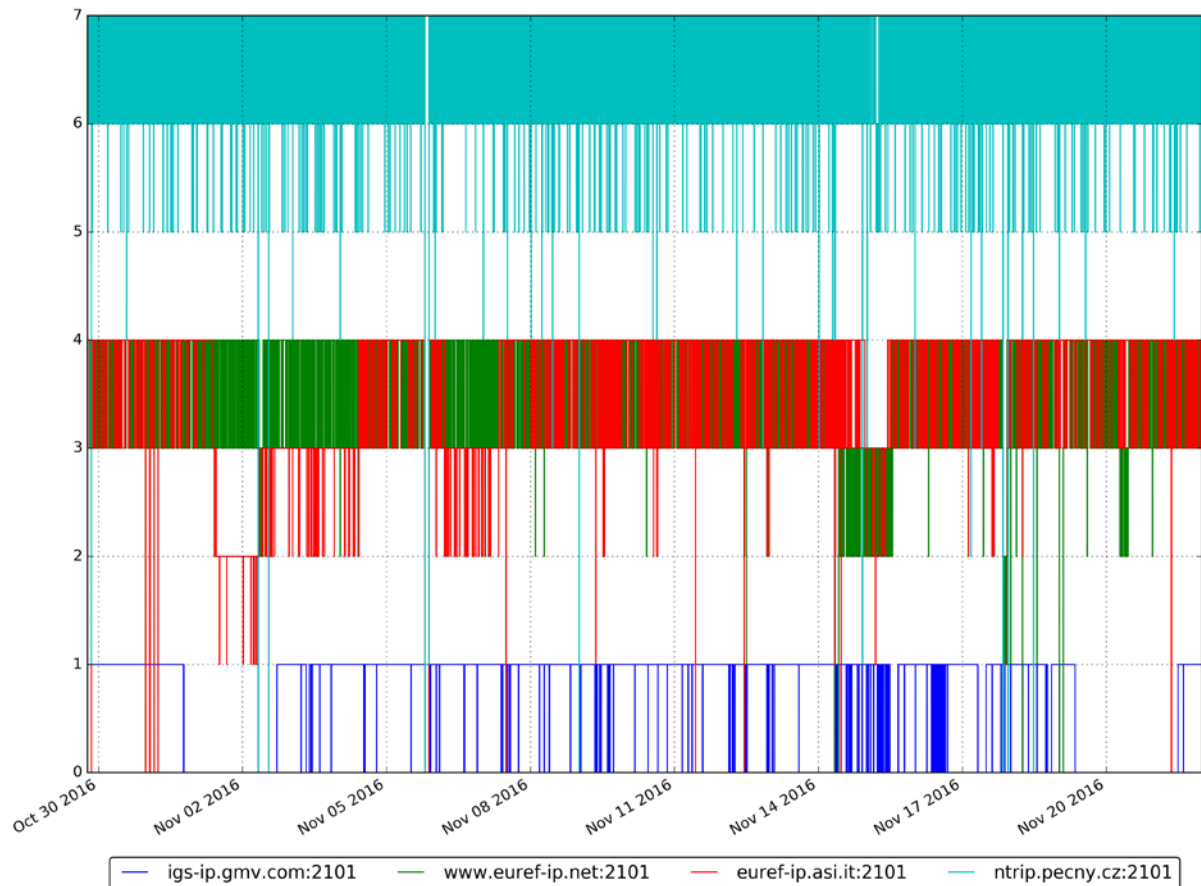
Figure 2.9: Availability test on the global GNSS RT acquisition for all epochs in days between 304 and 326.

Taking into account the adopted availability thresholds in the above section (from deliverable D4.1), the performance is considered above the level of acceptance and close to the over-performance level, since the mean value of available datastreams is 15.32 out of 16. It is also worth mentioning that the baselines in AUDITOR network are shorter than necessary, so there is redundancy to enable WARTK. A lack of availability in several datastreams shall not be critical. Nonetheless, especially in the southern-most region, the geometry of the available stations streaming in real time could be improved in a future add-on.

2.4 TOMION SW pre-processing modules – improved design and implementation

2.4.1 Introduction

Regarding TOMION's pre-processing modules, two main improvements have been considered and they are already implemented.

On the one hand, the reference satellite is selected in advance, from the predicted ephemeris and accurate coordinates of the CPF receivers, from those showing the largest and common expected visibility time over 25 degrees of elevation. An example of its comparison with the observed visibility

can be seen in next figure, as far as the table containing the finally selected reference satellites during the same day.
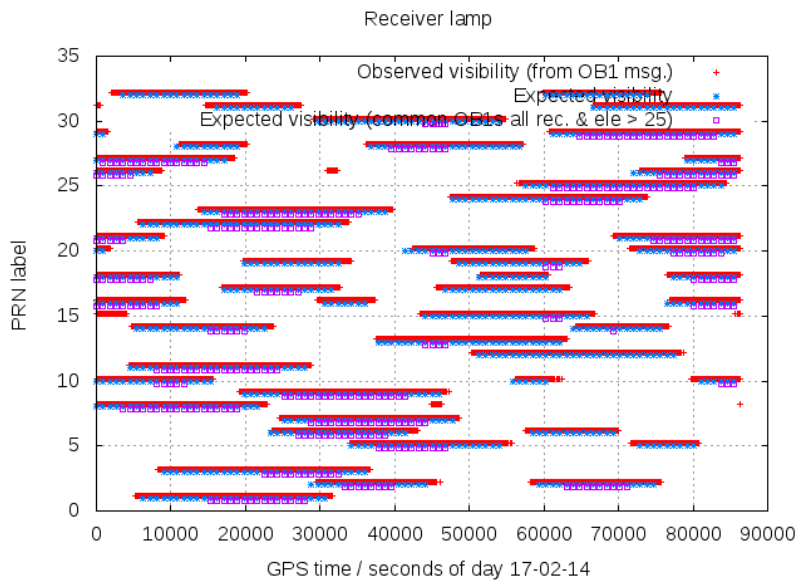
Figure 2.10: Example of Observed vs Expected visibility (for all the observations, and for the common ones above 25º) of GPS transmitters from LAMP permanent receiver (day 14 February 2017).

Table 1 Example of reference satellite selection performed for the AUDITOR RT-GNNS network for day 14 February 2017.

Initial GPS time / s	Final GPS time /s	ref. sat. PRN
0	10800	18
10800	25200	11
25200	45000	9
45000	61200	5
61200	71100	24
71100	86399	29

On the other hand, the cycle slip detection is mostly based on discontinuities of the geometry-free combination of the carrier phases (such as LI=L1-L2); the discontinuities of Melbourne-Wübbena combination are considered as well, as far as the option to flag them as well from the outlier in the pre-fit residual of the geometry-free combination of carrier phases, for permanent receivers with accurate apriori positions and tropospheric delay. The resulting cycle-slip detection is summarized, for the first 12 hours of day Feb 14th, 2017, in next figure, where the number identifying the continuous phase-arc for each transmitter-receiver pair, is represented vs time. It can be seen how this number

usually increases at the end and/or at the beginning of some arcs as expected due to the associated low elevations.
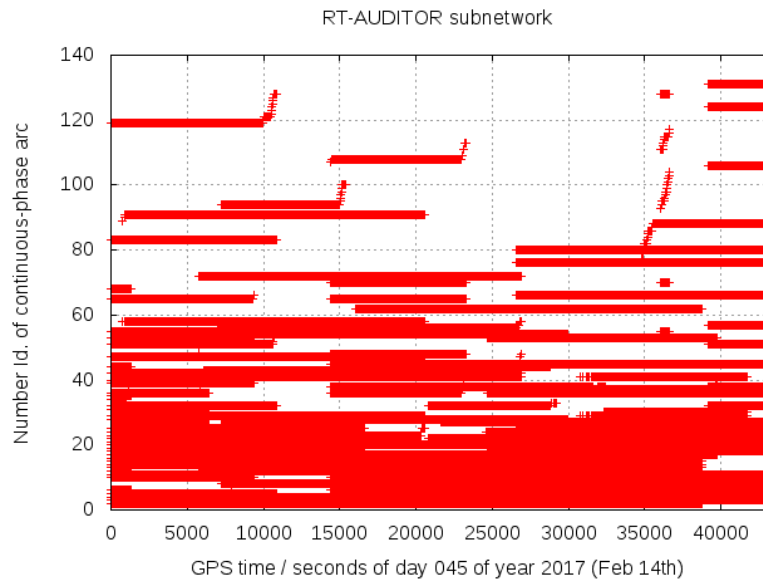
Figure 2.11: Example of the evolution of the integer Id of cycle slips vs time, for all the satellites in view from an AUDITOR subnetwork during the day 14 February 2017.

2.5 TOMION SW prefit module – improved design and implementation

2.5.1 Introduction

The prefit module allows to calculate the residuals between the measurements and the modelled terms before fitting all parameters to be estimated in TOMION's filter module, incorporating all the available apriori values and covariances within the Jacobian (e.g. design) matrix associated to the model. In this way, all known parameters or the best-known estimation of them can be subtracted to the observables. As part of the prefit module, clocks, geometry, troposphere and ionosphere can be modelled depending on the adopted strategy (absolute, or relative –as in AUDITOR's case-). In addition, an optional new feature has been implemented to take into account at this stage (prefits) the double differences of the ambiguities $\nabla\Delta B_c$ and $\nabla\Delta B_w$ and fixing them when possible (*we exclude $\nabla\Delta B_I$ in order to avoid to rely on any apriori ionospheric model)* This minimizes the number of unknowns associated to the ambiguity terms that need to be estimated in the filter (see Section 2.5.2 for the details, where we show one example of it, besides an example of the more conventional ambiguity fixing after the filter).

2.5.2 Ambiguity fixing

A typical example of the look of the triple-differences (top; i.e. taking into account differences in time as well) and double-differences referred to the fixed value (bottom) of the prefit residuals, for the three ambiguities (columns), is shown in next two figures, vs time and vs elevation respectively (Feb. 13th, 2017, in the RT-AUDITOR subnetwork).
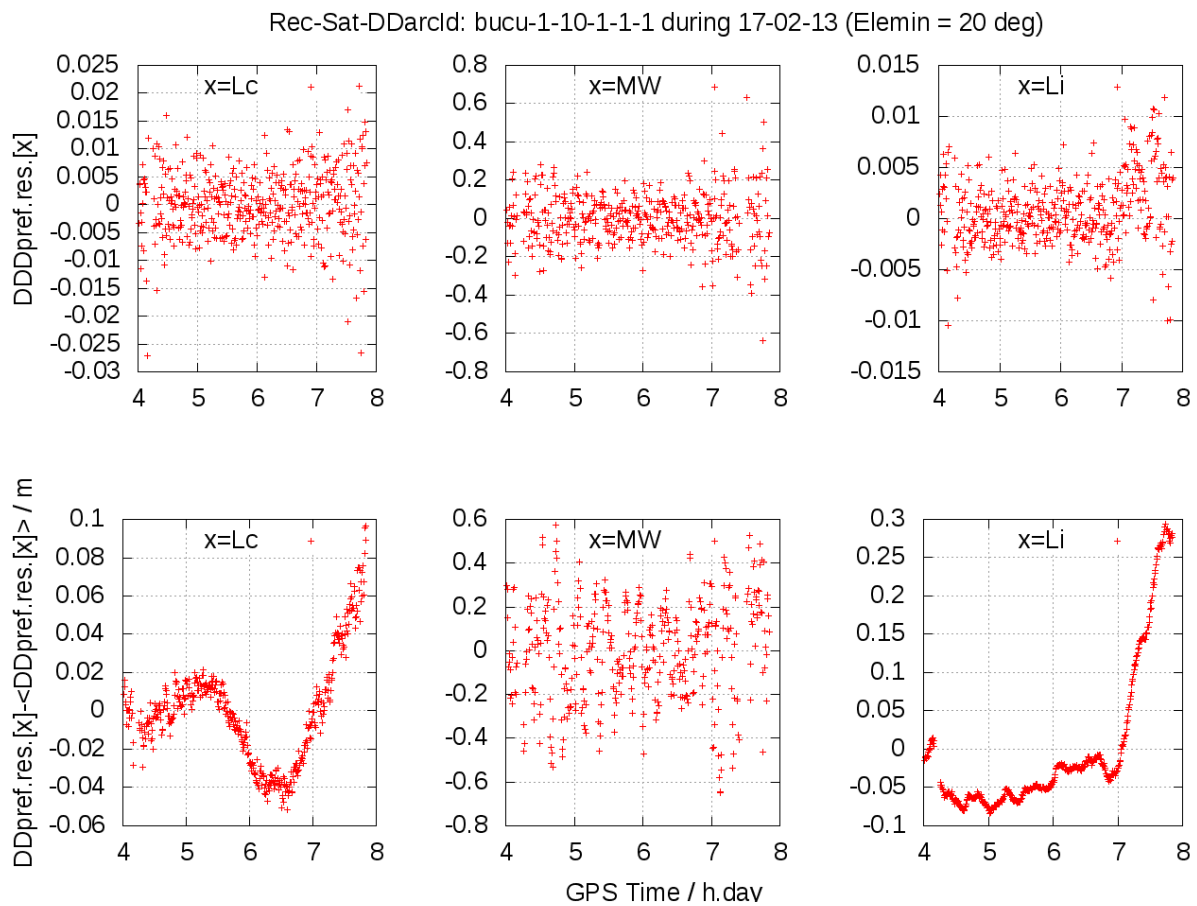
Figure 2.12: Example of the time evolution of the triple-differences (first row) and double-differences regarding to the average value (second row), for the ionospheric-free, Melbourne-Wubbena and geometric-free (ionospheric) combinations (first, second and third columns respectively). This corresponds to the GPS satellite PRN1 the day February 13th, 2017.
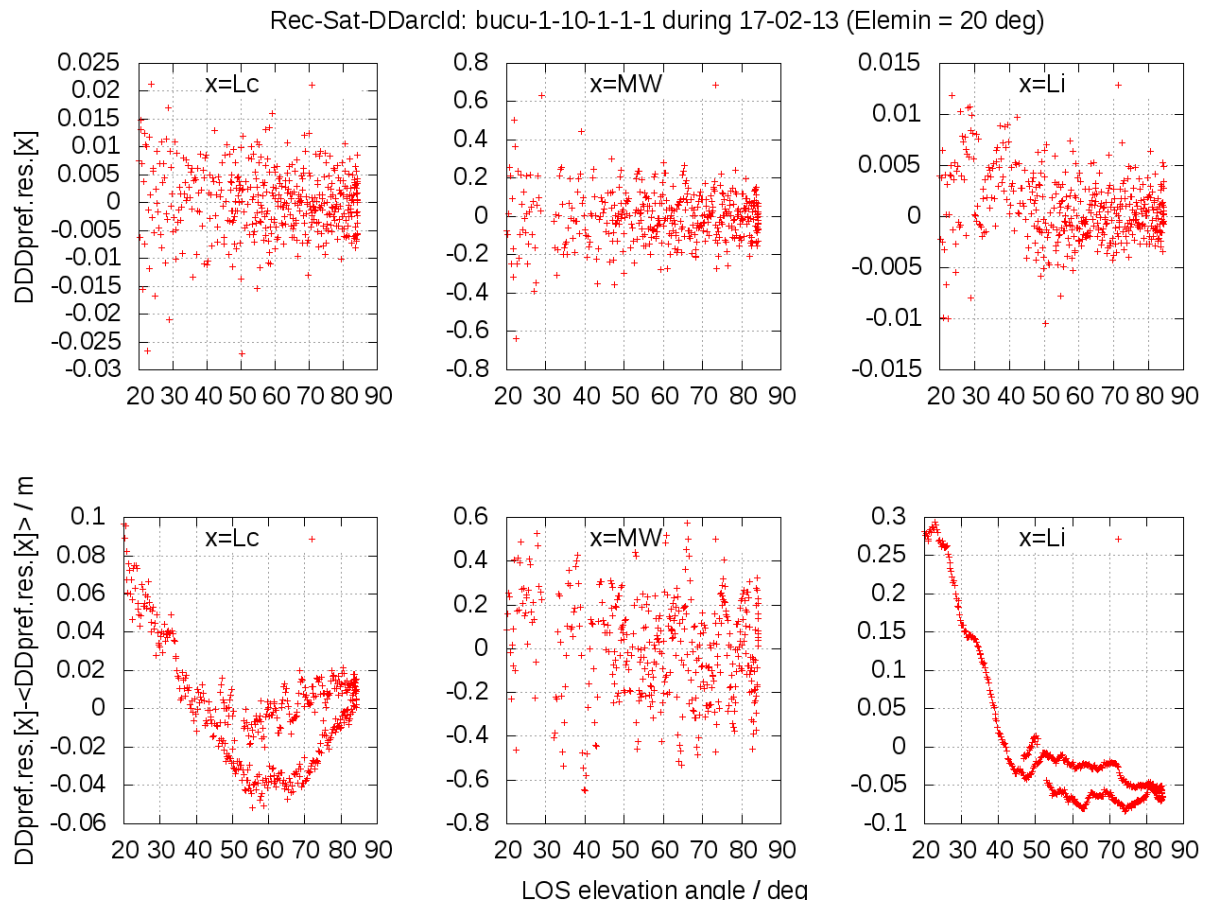
Figure 2.13: Example of the elevation dependence of the triple-differences (first row) and double-differences regarding to the average value (second row), for the ionospheric-free, Melbourne-Wubbena and geometric-free (ionospheric) combinations (first, second and third columns respectively). This corresponds to the GPS satellite PRN1 the day February 13th, 2017 (like previous figure).

As an example of the second (optional as well) double-differenced ambiguity fixing scheme implemented in the CPF from the filter, the next three plots show an example corresponding to the double differenced carrier phase ambiguities for ionospheric-free, wide-lane and ionospheric carrier phase biases for IGS stations (in red the floated values provided by the filter and in the green the fixed value).
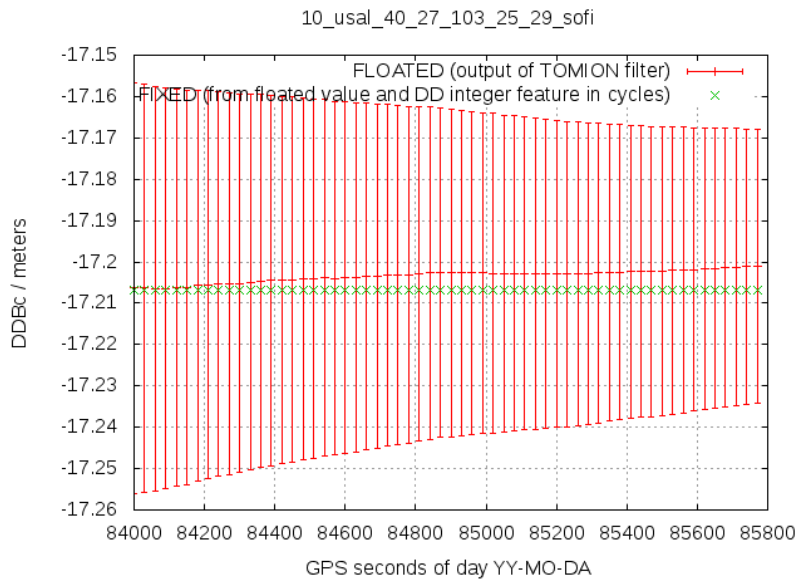
Figure 2.14: Example of the double differenced carrier phase ambiguity for ionospheric-free carrier phase biases (in red the floated values provided by the filter and in the green the fixed value, GPS satellite PRN 10 observed from USAL, day February 13th, 2017).
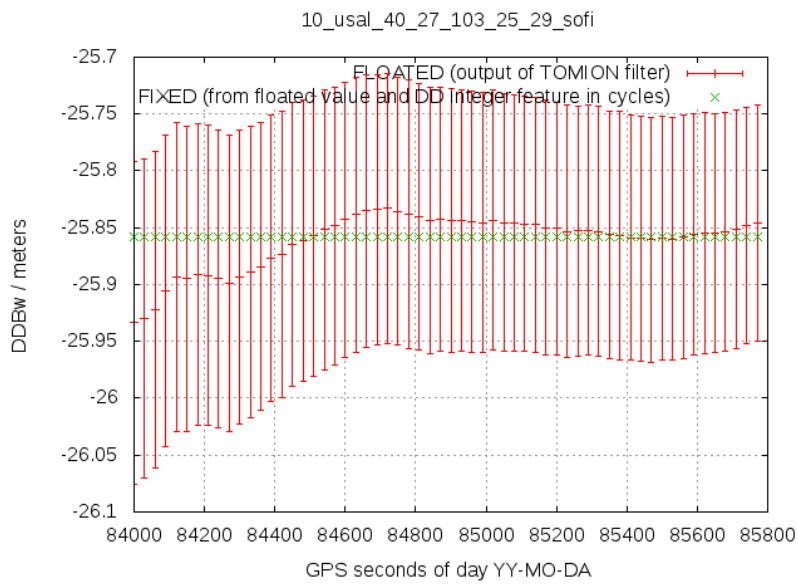
Figure 2.15: Example of the double differenced carrier phase ambiguity for wide-lane carrier phase biases (in red the floated values provided by the filter and in the green the fixed value, GPS satellite PRN 10 observed from USAL, day February 13th, 2017).
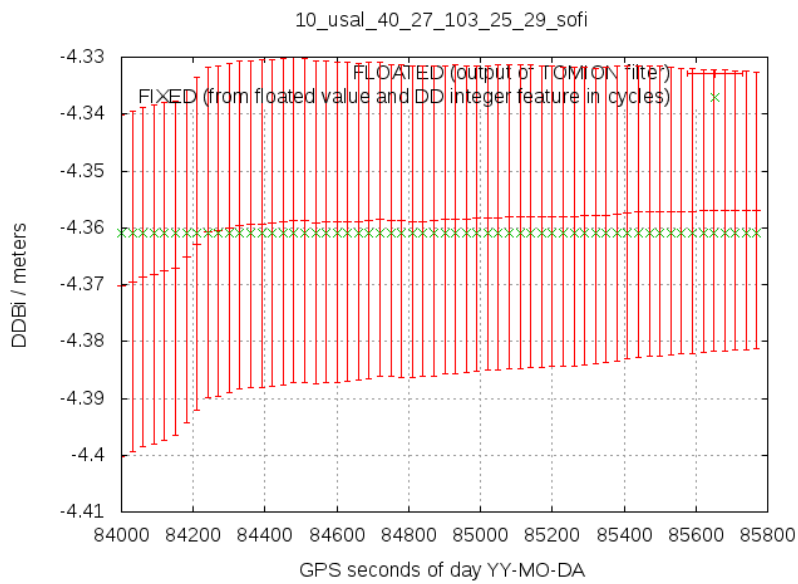
Figure 2.16: Example of the double differenced carrier phase ambiguity for ionospheric carrier phase biases (in red the floated values provided by the filter and in the green the fixed value, GPS satellite PRN 10 observed from USAL, day February 13ᵗʰ, 2017).

In order to enable fixing these ambiguities, an updated approach is considered based on the following equations:

$$2\nabla\Delta B_c = [\underbrace{\lambda_w \nabla\Delta \overbrace{N_w}^{N_1 - N_2}}_{\widehat{\nabla\Delta B_w}} + \lambda_n \nabla\Delta \overbrace{N_n}^{N_1 + N_2}]$$

$$\widehat{\nabla\Delta N_n} \Rightarrow \nabla\Delta N_1 \quad \nabla\Delta N_2 \Rightarrow \frac{\nabla\Delta STEC}{\nabla\Delta B_c}$$

In the first equation, it is written the relationship between the double-differenced ionospheric-free ambiguity and the double differenced wide-lane and narrow-lane ambiguities. The fact is that the double-differenced $\nabla\Delta B_c$, can be computed accurately thanks to very accurate modelling and knowledge of the permanent receiver position, by rounding the floated solutions (given the wide-lane wavelength) after the convergence time of some minutes. In parallel, fixing the double-difference of the wide-lane ambiguity carrier-phase, $\nabla\Delta B_w$, can be performed after few minutes of convergence due to both, the ionospheric- and geometry- free nature, and the reduced pseudorange noise of the Melbourne-Wübbena combination. Afterwards it is possible to typically fix the narrow-lane ambiguity (from both $\nabla\Delta B_c$ and $\nabla\Delta B_w$, once the "parity check" is fulfilled, i.e. $\nabla\Delta N_w + \nabla\Delta N_n$ must be an even number), and thus, we can derive the double-differenced terms $\nabla\Delta N_1$ and $\nabla\Delta N_2$, which account for the

double-differences of the carrier-phase ambiguities for frequencies f_1 and f_2, respectively. The subsequent step is to fix the $\nabla\Delta B_c$ to derive very accurate double-differences of the slant Total Electron Content, $\nabla\Delta STEC,$ corresponding to both $\nabla\Delta N_1$ and $\nabla\Delta N_2$.

These ambiguity fixing approaches (from the prefits and/or from the filter output) enable to provide feedback to the prefit module from the filter outputs. Removing the fixed double-differenced ambiguity terms enables to have better prefit residuals and a lower number of unknowns to be estimated in the filter, ideally under 100% of success of ambiguity fixing in a given epoch, from (m-1)*(n-1) to m+n unknowns corresponding to the ambiguities . In this regard, more details are provided in Section 2.7.

2.5.3   Improvements on the tropospheric delay model

As it is explained in detail in Graffigna, 2017 [14], co-author of this deliverable, the TOMION SW supports the possibility to compute a-priori Zenith Tropospheric Delays (ZTDs) with two different tropospheric mapping functions. The Niell Mapping Functions (NMF; see Niell, 1996 [11]), which was already implemented, and the Vienna Mapping Functions (VMF), which has implied a SW upgrade in the frame of AUDITOR's first year.

In the case of the classical Niell implementation, the Zenith Hydrostatic Delay is computed with Saastamoinen and the Zenith Wet Delay *a priori* is constant and equal to 10 cm. Both two quantities multiplied by its respective NMF (i.e. the hydrostatic and wet), amount to the a-priori ZTD used within the prefit module*.*

In Bohm et al., 2015 [13], an improved empirical model for the tropospheric slant delay was presented that can be used as an a-priori value within the prefit module. In addition, a subroutine called GPT2w has been retrieved from their website to calculate meteorological parameters such as pressure, temperature, temperature lapse rate, mean temperature of the water vapor, water vapor pressure, hydrostatic and wet mapping function coefficients a_h and a_w, water vapor decrease factor and geoid undulation for specific sites near the Earth surface. These values allow to compute both wet and dry ZTDs at these locations and thus derive the Vienna Mapping functions.

In order to validate the obtained results on TOMION's ZTDs estimates, we have considered two independent references. On the one hand, the International GNSS Service (IGS) final product for such term, which are available through IGS sites. On the other hand, we have also computed a direct estimation from GIPSY/OASIS-II, reference software from the Jet Propulsion Laboratory (JPL, NASA), considering the same input conditions. For additional details, please refer to Graffigna, 2017 [14].

2.6 TOMION SW prefit module – performance evaluation

The performance evaluation of the prefit module has been carried out in different sensitive aspects of the modelling. This includes, among others, the precise coordinates estimated for the permanent

receivers, compared with the ones computed from IGS analysis centers; this computation has to be done only time to time, and in post-processing (see next two plots for two receivers at the target area, including the convergence toward the external reference IGS values). The companion results for the estimated zenith tropospheric delay, showing its well agreement in standard deviation with IGS, is also shown in the following two plots (the bias regarding IGS is not present when compared with GIPSY results; see Graffigna 2017 and the following plots below).
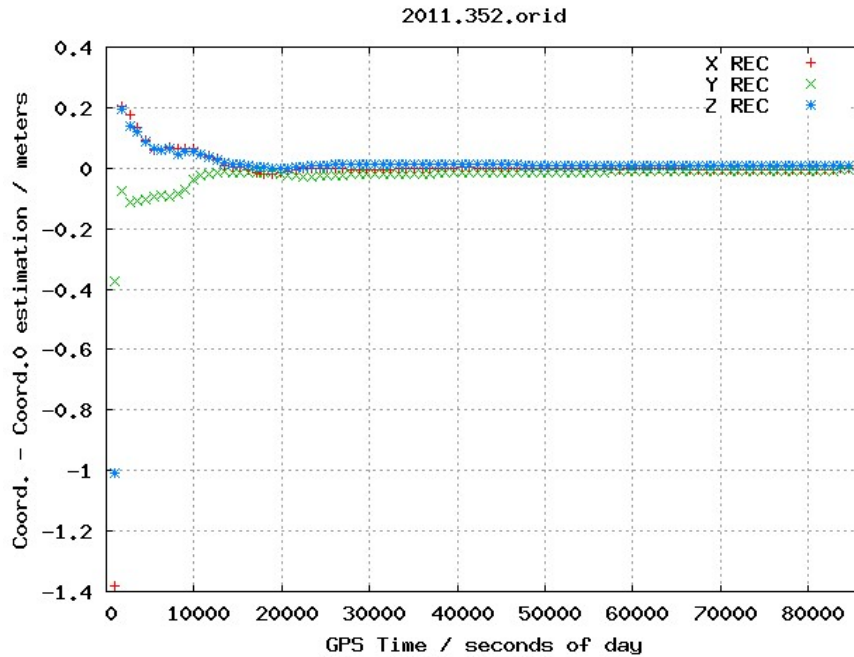
Figure 2.17: Computed coordinates by AUDITOR TOMION for orid receiver wrt IGS
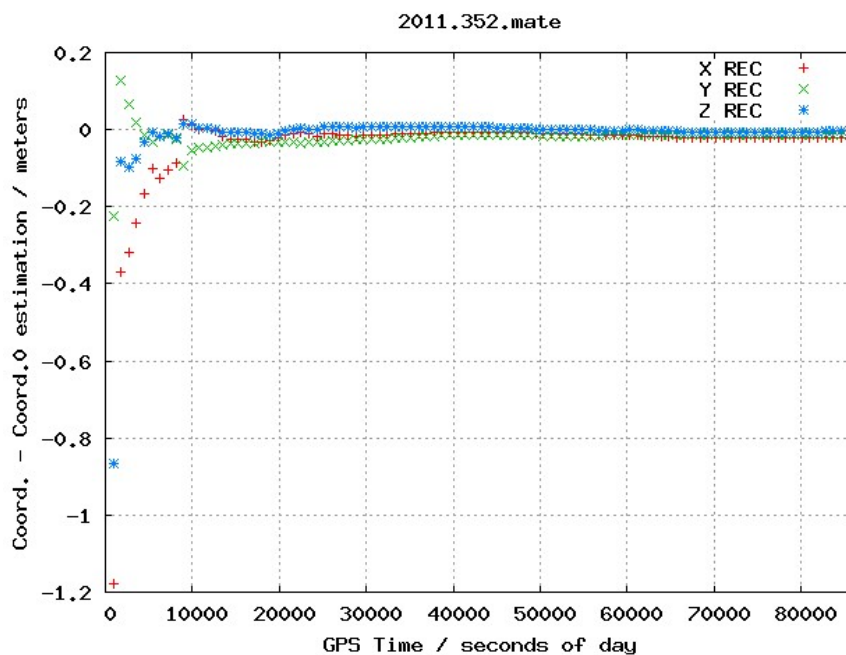
Figure 2.18: Computed coordinates by AUDITOR TOMION for mate receiver wrt IGS
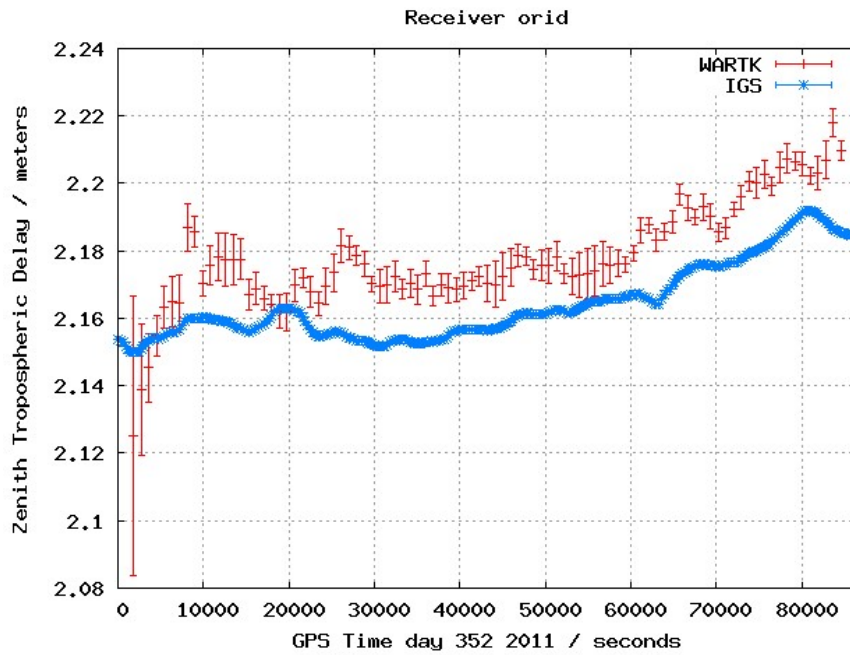
Figure 2.19: Troposphere estimation for orid receiver vs IGS (352, 2011)
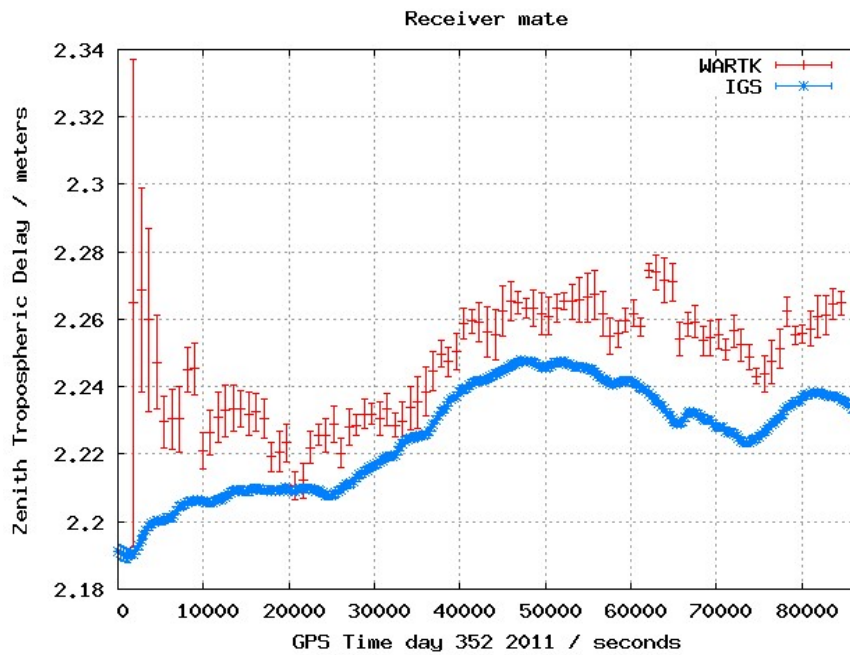
Figure 2.20: Troposphere estimation for mate receiver vs IGS (352, 2011)

2.7 TOMION SW filter module – improved design and implementation

Complementing the description provided in Section 2.5.2, the RT-TOMION SW filter module has been improved providing new feedback to the prefits module on two main points:

1) The double-differenced ambiguity fixing is now performed exactly, by removing the double-differenced ambiguities, from the best estimated ambiguities in the filter, from the unknowns (and not as a filter constraint like before):

$$B_i^j = \Delta \nabla B_i^j + B_i^0 + B_0^j - B_0^0$$

where the carrier phase ambiguity of satellite j measured from receiver i, B_i^j (for each given combination, for instance B_c for the ionospheric-free one) can be expressed in terms of the ambiguities of the reference satellite seen from the permanent receiver, B_i^0, of the given satellite from the reference receiver, B_0^j, and in terms of the ambiguity of the reference satellite seen from the reference receiver, B_0^0, once the double-differenced ambiguity ($\Delta \nabla B_i^j$) is subtracted from the corresponding prefit. In this way, the number of unknowns for the line-of-sights successfully fixed is decreased from (m-1)*(n-1) up to m+n, whan all possible double-differenced ambiguities for the m satellites and n receivers are fixed.

2) New outlier detection strategy from the output of the filter which allows to remove few large prefits when they might be introducing an unexpected large error.

2.8 TOMION SW filter module – performance evaluation

2.8.1 Troposphere estimation validation wrt IGS and GIPSY

It can be seen in Figure 2.17 and Figure 2.18, for receivers MATE and BUCU, the good agreement in the ZTD bias of TOMION with respect to GIPSY, and different in about one centimeter regarding to IGS (more details can be found in Graffigna, 2017).

Receiver MATE 353

Figure 2.21: Troposphere estimation for mate receiver with TOMION (WARTK) vs IGS vs GIPSY (353, 2011)

Receiver BUCU 353

Figure 2.22: Troposphere estimation for bucu receiver with TOMION (WARTK) vs IGS vs GIPSY (353, 2011)

2.9 Communication with the user GNSS receivers – Data format

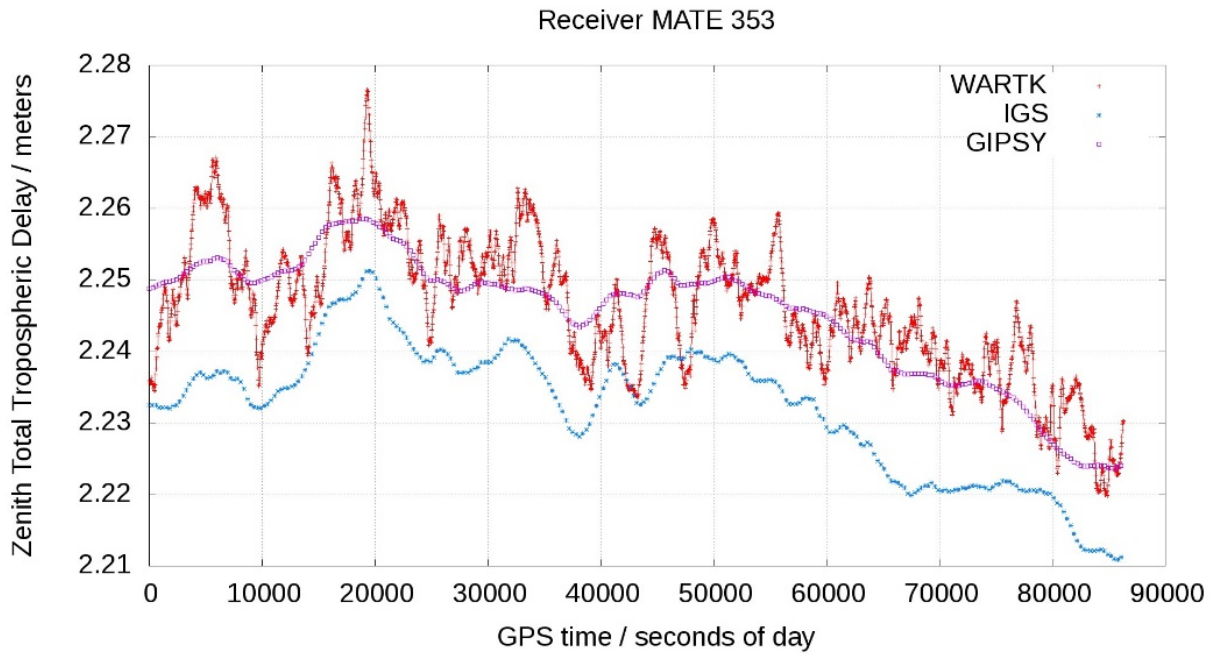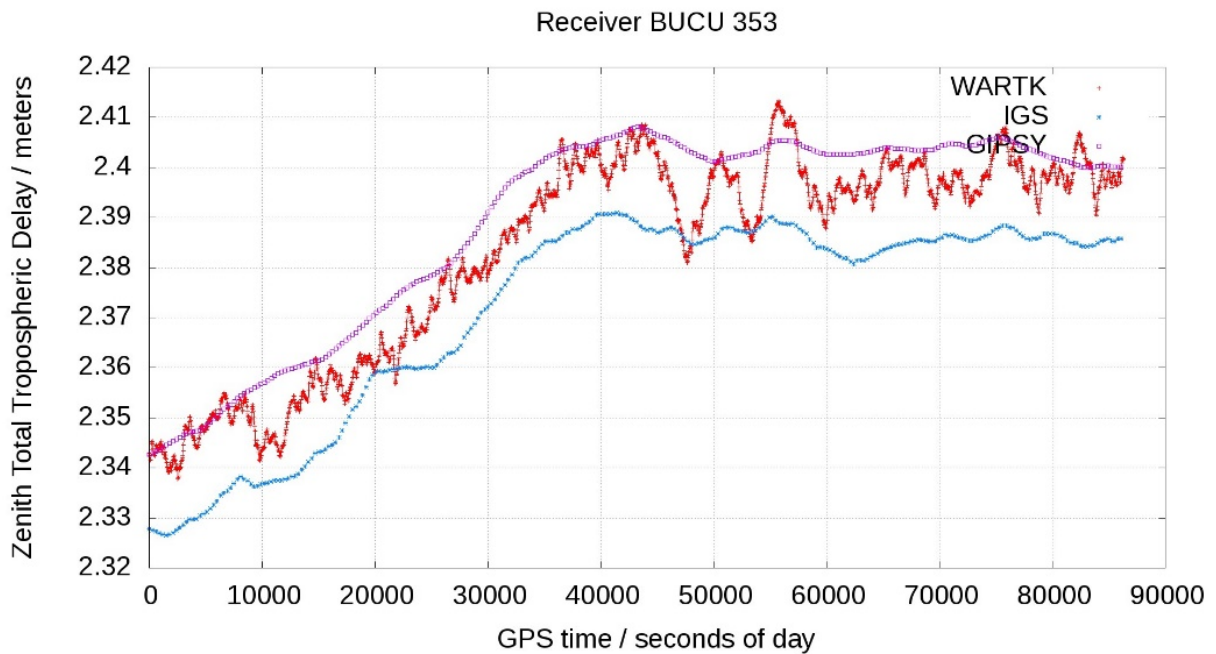In the literature, one can identify several possibilities –some of them currently under development or discussion– to disseminate in real time (or near real time) VTEC and/or STEC data (either regional/global maps or corrections) to the users. These are summarized in Table 2, with relevant comments in each case.

Table 2 VTEC/STEC formats supporting real-time

Data format	Advantages	Disadvantages	Remarks
RTCM SSR (MT-10; SH)	Open Standard recommended by the Radio Technical Commission for Maritime Services (RTCM). BKG NTRIP SW supports it. In general, RTCM messages are widely used.	Spherical Harmonics are not suitable to all approaches so it can imply lower quality data than the original.	CNES is the only center distributing their VTEC maps based on this format. IGS RT-WG promotes the dissemination of messages based on RTCM standards.
RTCM SSR (MT-11)	Open Standard recommended by the Radio Technical Commission for Maritime Services (RTCM).	Limited information found. May probably be a message still under discussion.	
EGNOS GIVD GIVE messages (message types 18/26).	Easy to access (FTP protocol). Integrity.	Not open-standard. No SW availability. Variable messages. Need to define new specific messages for new RT products.	ftp://ems.estec.esa.int UPC developed a decoder in JAVA
Net-CDF	Flexibility. Integrity. Programs are available in many programming languages to easy its use. Used in the scientific community.	RT capability seems not well documented (NRT seems feasible).	Used by entities world-wide such as ESA, EUMETSAT, NASA, NOAA, CDDAC, etc.
IONEX via FTP	Common-used format for VTEC maps. Easy for users to retrieve data without additional SW.	NRT rather than RT. Latency issues. Not thought for streaming. User side should query the FTP continuously.	
(**STEC**) Simon Banville	Takes into account specific features on STECs dissemination.	Not an standard. Evolving. Currently: No integrity. Not built for real time streaming (header, time tags refered to start time in the header, postprocessing site names of 4 letters). Values provided in	https://www.blackdotgnss.com/2017/01/27/exchanging-stec-data (also including comments)

		format "F10.4" may not provide enough accuracy.	

In addition, the following formats within AUDITOR consortium are also considered:

- The **WARTK-DSM** message containing an accurate slant TEC model per satellite (generalized as **WARTK-DS2** message; see below)

- **DGFI-TUM** format to encapsulate their maps.

- A new possibility on AUDITOR message to support the precise GNSS navigation has been identified, based on distributing global accurate real time VTEC GIMs (in **IONEX** format) **+ BIM** (fixed coefficients), to be applied by the user.

An analysis to check the most appropriate format is envisaged in the integration phase, as commented in MTR meeting. In any case, the baseline approach is to consider the formats within the Consortium to have full control in a first stage. Also note that the different options for dissemination in Table 2 are still not consolidated in the scientific community and may still be subject to discussion. These cases together with the most feasible options in Table 2 are explained in more detail in next subsections.

2.9.1 RTCM VTEC message in Spherical Harmonics (message 1264)

We already checked several possibilities on the way to encode the VTEC values to RTCM3 format before being transmitted to AUDITOR users. As per existing tools:

- RTKLIB rtcm3e.c source code implements this for multiple RTCM messages. Nonetheless, it does not support encoding message 1264 on VTEC Spherical Harmonics.

- SAPOS GNSS Surfer also implements encoding routines but has been discarded as it is only supported in Windows (x64). The use of Wine or similar programs to run Windows programs under Linux environments is not considered practical nor robust enough.

As it was expected, given the novelty of the VTEC SH RTCM messages, the development of a tool to encode VTEC SH coefficients in RTCM3 standard is also a possibility within AUDITOR implementation phase. At the moment, the update of RTKLIB's rtcm3.c and rtcm3e.c is still a possibility.

For such a purpose, it might be useful one RTCM 3.2 file UPC-IonSAT has been given as reference for implementing the message type 1264 on VTEC in SH. It is remarkable that this file must be kept confidential, as requested by the provider.

Table 3 RTCM messages (including SSR proposed ones; extracted from [3])

System/ RTCM SSR Message (* proposed)	GPS	GLONASS	Galileo	SBAS	QZSS	BDS
Orbits	1057	1063	1240*	1246*	1252	1258*
Clocks	1058	1064	1241*	1247*	1253*	1259*
Code Biases	1059	1065	1242*	1248*	1254*	1260*
Combined Orbits and Clocks	1060	1066	1243*	1249*	1255*	1261*
VTEC	1264*					
Phase Biases	1265*	1266*	1267*	1268*	1269*	1270*

2.9.2 RTCM VTEC message

In http://www.geopp.com/pdf/gpp_ppprtk12_msg_f.pdf, it is written that another potential RTCM VTEC message (labelled MT+11) is also being considered. As stated in the above link, this message would provide a grided higher resolution model (regional/continental densification) to be added on top of RTCM SH message.

The possibility that this message could be useful to disseminate global maps directly, without the need of a Spherical Harmonic VTEC message, would need to be checked.

2.9.3 WARTK DSM/DS2 messages

This is the most direct way to disseminate the messages since these were formerly implemented and have been operational for a certain time (up to one year). Note that DSM messages, directly providing an STEC model per satellite, have been generated continuously and/or for certain test campaigns in some European projects.

Regarding DS2 messages, these are a generalization of DSM ones. The update allows to allow defining the point where the planar fit is considered, no need to be associated to the reference receiver ionospheric pierce point (for each given satellite in view). This flexibility can further improve the interpolation of the STEC determination around the user, minimizing the residuals of the planar fit since the user IPPs would be in the vicinity.

2.9.4   DGFI-TUM B-Spline-messages

From the DGFI-TUM side, as it was commented in D4.1, ionospheric corrections are calculated by uniform- and non-uniform B-Spline (BS) functions. The main objective for this approach is the possibility to consider densification areas of interest for which a sufficient number of observations is available. In other words, with this approach it will be possible to model ionospheric information with a high spectral and spatial resolution for certain regions.

For setting up a message based on BS modelling there are basically two options, namely providing (1) VTEC BS coefficients or (2) VTEC grid values.

In the case (1) an encoder procedure for these coefficients is necessary, because the user has to evaluate the BS model just as in the spherical harmonic case, only substituting the B-splines for the spherical harmonics. In case of option (2) either global VTEC grid values or the combination of global and regional VTEC grid values will be disseminated to the user. The latter, i.e. the combination of global and regional grid values, will be provided if the user needs corrections for regional applications with a higher spatial resolution in certain densification areas.

Since the option (2) seems to be easier to handle we prefer to implement a message based on VTEC grid values for global and regional applications.

Further details to be provided in next reports.

2.9.5   IONEX format - Global real time GIMs maps & BIM

On the one hand, the computation of real time GIMs based on the new implementation at chapman.upc.es has been resumed successfully so that global real time maps (labelled URTG) are being computed at the moment and made available through the following link: http://chapman.upc.es/tomion/real-time/quick/last_results

Note that the real time VTEC (and standard deviation) maps are being computed in test mode at the moment to make sure they are properly generated in the new server. Examples on these maps are shown in Figures 2.19 and 2.20 below (note that animations are also provided in the link above).
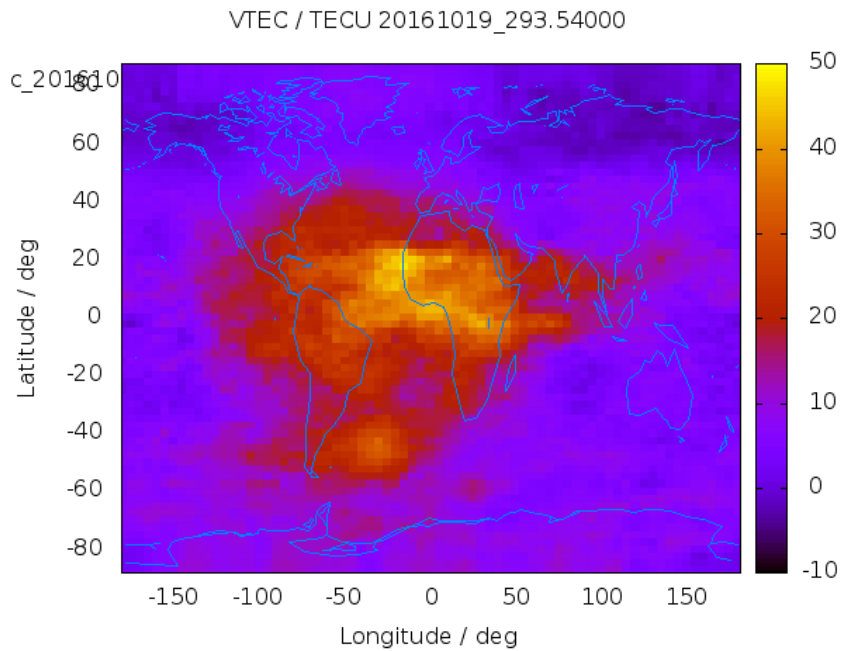
**Figure 2.23: Real time VTEC global ionospheric map (from the temporal link
http://chapman.upc.es/tomion/real-time/quick/last_results/urtg16293.1500.tec0.global.gif)**
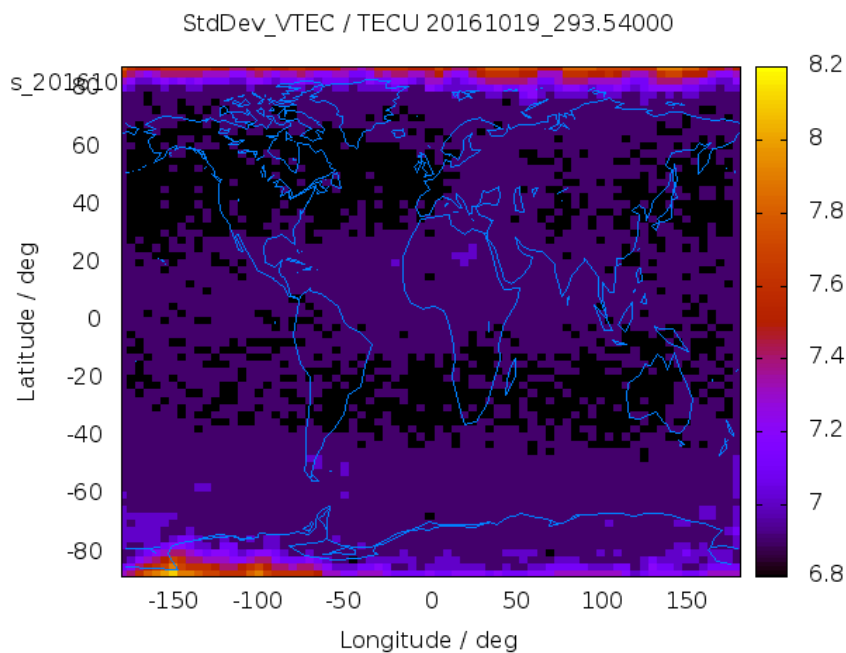
**Figure 2.24: Std. dev. of real time VTEC global ionospheric map (from the temporal link
http://chapman.upc.es/tomion/real-time/quick/last_results/urtg16293.1500.rms0.global.gif)**

On the other hand, Barcelona Ionospheric Mapping (BIM) function maps could be provided to improve the STECs determination for each receiver-satellite ray at the user side based on VTEC values of the GIM. In MTR meeting, it was decided to assess this possibility together with the other options, as part of Task T5.4. Last but not least, the details on the BIM are provided in Deliverable D4.2.

2.10 AUDITOR messages dissemination – verification

The communication system between the CPF corrections and the GNSS software receiver needs to be ready for the following tests numbered within D1.3 Test definition:

> 6.51 Test – AUDITOR's Message generation and retrieval
>
> 6.52 Test – AUDITOR corrections: Controlled environment.
>
> 6.53 Test – AUDITOR corrections: real data
>
> 6.55 Test – Triggering of SRMTID warnings
>
> 6.56 Test – Positioning with SRMTID

We can mention that, to run first tests, it is envisaged to test the dissemination of WARTK AUDITOR messages by means of SNIP NTRIP caster, Beta version for Ubuntu 16.04 (see https://www.use-snip.com/). This is a free NTRIP caster allowing for three simultaneous data streams and unlimited client connections for a one-hour period each time SNIP is started.

The use of SNIP is important to test AUDITOR system in a realistic scenario linking the CPF network host at the iBOGART Cloud with any potential AUDITOR user (GNSS software receiver shall be available for this test). Note that all features are given in the free SNIP caster. Nonetheless, at a later stage in order to run the commercial application, SNIP will need to be upgraded to a full version. As an alternative, there is also the possibility to use BKG Professional NTRIP caster. Unfortunately, both options are not open-source solutions.

As a back-up option, there is the possibility to use a simple TCP/IP connection. For this purpose, netcat (nc) has been identified or directly the BNC utility for this purpose. Also there is the possibility to establish a dedicated FTP service for first tests on dissemination.

Note that the dissemination approach will be tested as part of the integration activities within AUDITOR WP6.

3. Conclusions

In this document, the design of the iBOGART network modules have been outlined as well as implementation issues and validation steps carried out prior to their integration. In this context, we have provided inputs on the RT-GNSS data gathering module, the main components of TOMION's SW, including the pre-processing steps, prefit module and filter module, which have been consolidated in the frame of AUDITOR activity. Furthermore, communication aspects have been discussed considering a new option by the combined use of GIMs and Barcelona Ionospheric Mapping function (BIM).

3. Conclusions

4. References

[1] Hernández-Pajares M., J.M. Juan, J. Sanz, O. Colombo, "Application of ionospheric tomography to real-time GPS carrier-phase ambiguities resolution, at scales of 400-1000 km and with high geomagnetic activity", Geophysical Research Letters Vol. 27(13), pp. 2009-2012, 2000.

[2] Feltens, J., Angling, M., Jackson-Booth, N., Jakowski, N., Hoque, M., Hernández-Pajares, M., ... & Zandbergen, R. (2011). Comparative testing of four ionospheric models driven with GPS measurements. Radio Science, 46(6).

[3] Axel Rülke, Loukis Agrotis, Werner Enderle, Ken MacLeod, Oral presentation at IGS Workshop February 2016, Sidney, Australia (publicly accessible through http://www.igs.org/assets/pdf/W2016%20-%20PY0401%20-%20Rulke.pdf)

[4] Hernández-Pajares M, Wielgosz P, Paziewski J, Krypiak-Gregorczyk A, Krukowska M, Stepniak K, Kaplon J, Hadas T, Sosnica K, Bosy J, Orús-Pérez R, Monte-Moreno E, Yang H, García-Rigo A, Olivares-Pulido G. (2016) Direct MSTID mitigation in precise GPS processing, submitted to Radio Science.

[5] Hernández-Pajares M, Juan JM, Sanz J, Aragón-Àngel A (2012). Propagation of medium scale traveling ionospheric disturbances at different latitudes and solar cycle conditions. Radio Science, 47(6).

[6] Hernández-Pajares, M., Juan, J. M., & Sanz, J. (2006b). Medium-scale traveling ionospheric disturbances affecting GPS measurements: Spatial and temporal analysis. Journal of Geophysical Research: Space Physics (1978-2012), 111(A7).

[7] Husin, A., M. Abdullah, & M. A. Momani (2011), Observation of medium-scale traveling ionospheric disturbances over Peninsular Malaysia based on IPP trajectories, Radio Sci., 46, RS2018, doi:10.1029/2010RS004408

[8] Hernández-Pajares, M. (2013), Analysis of the ionospheric signatures before, during and after the Fukushima earthquake, IPRESES project, UPC, Sep. 2013.

[9] Tsugawa, T., Otsuka, Y., Coster, A. J., & Saito, A. (2007b). Medium-scale traveling ionospheric disturbances detected with dense and wide TEC maps over North America. Geophysical Research Letters, 34(22).

[10] Hernández-Pajares, M., Juan, J. M., & Sanz, J. (1999). New approaches in global ionospheric determination using ground GPS data. Journal of Atmospheric and Solar-Terrestrial Physics, 61(16), 1237-1247.

[11] Niell, A. (1996). Global mapping functions for the atmosphere delay at radio wavelengths. *Journal of Geophysical Research: Solid Earth*, 101(B2):3227–3246. 4, 28

[12] Orús, R., Hernández-Pajares, M., Juan, J. M., & Sanz, J. (2005). Improvement of global ionospheric VTEC maps by using kriging interpolation technique. Journal of Atmospheric and Solar-Terrestrial Physics, 67(16), 1598-1609.

[13] Böhm, J., Möller, G., Schindelegger, M., Pain, G., and Weber, R. (2015). Development of an improved empirical model for slant delays in the troposphere (gpt2w). GPS Solutions, 19(3):433–441. 8, 9, 28

[14] Graffigna, Victoria (2017). Consistency of different tropospheric models and mapping functions for precise GNSS processing. Master Thesis in Aerospace Science and Technology. February 6, 2017.